POLAR WARMING IN THE MARTIAN ATMOSPHERE: AN ANALYSIS OF DATA FROM MODERN SPACECRAFT

T. McDunn and S. Bougher, *Department of AOSS, University of Michigan, Ann Arbor, MI, USA (tmcdunn@umich.edu)*; **A. Kleinböhl,** *Jet Propulsion Laboratory, Pasadena, CA, USA*; **F. Forget**, *CNRS, Laboratoire de Météorologie Dynamique, Paris, France.*

Introduction: Polar Warming (PW) is a middle-to-upper atmosphere dynamical feature caused by the global circulation. It has been observed [e.g., 1-9] and modeled [e.g., 4, 5, 10-14] in the middle and upper atmosphere of Mars. In this paper we revisit the issue of PW in the Martian atmosphere and present a detailed characterization of the structure and evolution of this phenomenon seen in modern observations. We also present quantitative constraints for GCMs modeling the middle-to-upper atmosphere.

Defining PW: PW consists of a reversed latitudinal temperature gradient at the affected pressure levels. To-date, a community-wide definition of PW has not existed. In this paper, we define PW as:

$$\Delta T(p) = T_{hemispheric\ max}(p) - T_{eq\text{-}ward\ hemispheric\ min}(p)$$

That is, on a given pressure surface, the maximum temperature in a hemisphere, $T_{hemispheric\ max}(p)$, is identified and the minimum temperature equatorward of that maximum, $T_{eq\text{-}ward\ hemispheric\ min}(p)$, is identified; the difference of these quantities is the PW on that pressure surface in that hemisphere. We propose this definition be adopted by the community for the purpose of PW discussions.

Outstanding Questions About PW Climatology: As with other studies of Mars's atmosphere, the largest obstacle to the advancement of PW understanding has been data paucity. Previous observations did not provide the spatial or temporal resolution needed to adequately characterize the details of PW at Mars. Consequently, several important aspects of PW climatology remain unknown, such as: *Where precisely in the vertical does PW manifest at different seasons? Where in the vertical does it maximize? Where in the horizontal does it occur? Is the warming stronger during solstices or during equinoxes? Is it stronger during day or night? How far pole-ward does it extend during each season, at each pressure-level? How far equator-ward? How do the magnitude, horizontal, and vertical extent correlate with airborne dust observations? How do the minimum and maximum pressures at which warming manifests vary with season (distance from sun), with time of day (solar zenith angle), with solar cycle, and with lower-atmosphere dust loading?*

Over the past 12 years the paucity of data impeding advancement on these scientific questions has dissolved. Several spacecraft hosting instruments sampling a variety of atmospheric quantities have orbited or are presently orbiting the planet, providing a wealth of data applicable to these problems (characterizing PW at Mars and appropriately constraining GCMs in the middle-to-upper atmosphere domain). With the recent availability of these data, we recognize the time has come to re-visit the issue of PW at Mars and many of the above questions are addressed in this study.

Datasets: Five modern datasets in particular warrant re-visiting the PW phenomenon at Mars. The datasets come from the following instruments: Mars Climate Sounder (MCS) onboard NASA's Mars Reconnaissance Orbiter (MRO), Spectroscopy for the Investigation of the Characteristics of the Atmosphere of Mars (SPICAM) onboard ESA's Mars Express (MEx), and the accelerometer experiments (ACCEL) that flew on NASA's Mars Global Surveyor (MGS), 2001 Mars Odyssey (ODY), and MRO. Taken together, these datasets sample the Martian atmosphere from near the surface to ~1×10^{-6} Pa, all around the globe, over many seasons during several MarsYears (MY), and at different positions in the solar cycle. In this study we restrict our focus to pressures between 10 Pa (~ 30 km) and 1×10^{-4} Pa (~120 km) to address the task of characterizing the PW observed at Mars.

Constraints for Modeling: PW is a result of the global Hadley circulation. In the subsiding branch of the Hadley cell (above mid-to-high latitudes), adiabatic warming occurs, causing a reversal of the latitudinal temperature gradient one would expect from radiative considerations alone. This has been understood to be the driver of PW for sometime [e.g. 10, 11]. However, other aspects of PW formation remain less understood. *For instance, what governs the magnitude of the warming? What drives the warming to occur through a deeper layer of the atmosphere in some seasons than in others? What determines the pressure at which the warming will be maximized during any given season? What is responsible for a pole-ward or equator-ward extension of the warming? What roles do gravity waves, thermal tides, and dust-loading play in the magnitude and spatial extent of the warming?*

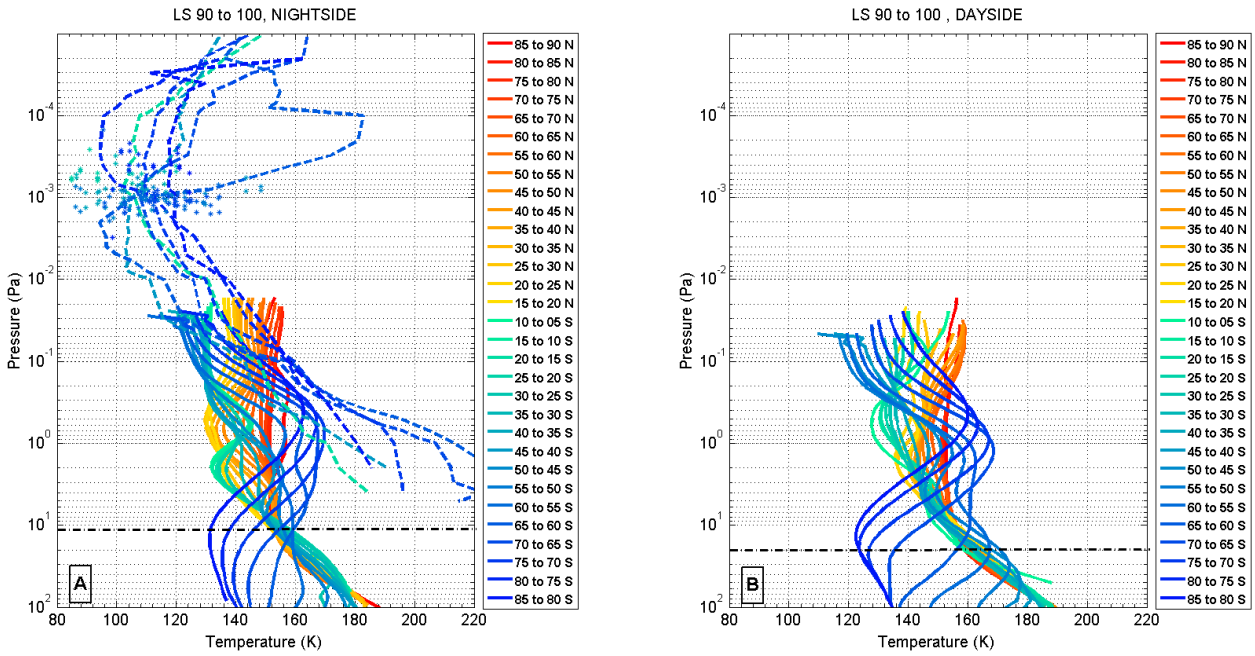

Figure 1. 5°-Latitude-bin-averaged observations of temperature at L_s 90-100°: (a) Nightside, LST = 1900 – 0500, (b) Dayside, LST = 0700 – 1700. See text for discussion.

Numerical models are the tools that can best address these questions; however before they can do so, they must be constrained and show that they are capable of reproducing the observed atmosphere. The final contribution of this paper is a set of quantitative constraints, based on the PW trends elucidated from observations, for GCMs to match in order to validate their middle-to-upper atmosphere calculations.

Sample of Results: Figure 1 shows 5°-Latitude-bin-averaged observations of temperature at L_s 90-100°. Panel A displays nightside (LST = 1900 – 0500) data while panel B displays dayside (LST = 0700 – 1700) data. The curves are color-coordinated according to latitude, with red corresponding to the summer (Northern) pole, yellow corresponding the summer low-latitudes, green corresponding to the winter low-latitudes and blue corresponding to the winter (Southern) pole. The solid curves are bin-averaged MCS (MY29) data while the dashed curves are bin-averaged SPICAM (MY27) data. Bin-averaged profile points having a bin-averaged uncertainty > 10 K have been removed. The stars represent MRO/ACCEL data (MY28). In the solid MCS curves in panel A we can clearly see warming into the winter pole beginning at pressures of 10 Pa and continuing to the top of the profile, p ~ 2.5×10^{-2} Pa. Also evident in the solid MCS curves of panel A is the pole-ward progression with height of $T_{hemispheric\ max}$ at this season. This is a pattern that persists throughout the Martian year. In the dashed curves we see winter high-latitudes exhibiting warmer temperatures than winter low-latitudes throughout the SPICAM profile (p ~ 2Pa up to 1×10^{-5}Pa). The ACCEL data also display evidence of PW. A final point we can take from panel A is the reasonable agreement between the datasets at this season, despite the different Martian years they observe.

Comparing panels A and B, we can see the diurnal variation of PW at this season. First, notice the downward movement of the 50° crossover point (that is, the pressure-level at which the winter mid-to-high-latitude curves first grow warmer than winter low-latitude curves), indicated by the black dash-dot-dash line. Next, notice that near the top of the dayside profiles, the low-latitude temperatures have once again grown warmer than the high-latitude temperatures. This is a departure from the trend observed on the nightside. Additionally, the low-latitude temperatures at the top of the dayside profile are significantly warmer than those seen at the top of the nightside profile. These diurnal variations in the observed PW are likely driven by the diurnal tide.

Figure 2 displays the data from Figure 1A in a different illustrative format. In this figure, the observed temperatures are shown versus latitude on constant-pressure surfaces. Black points represent MCS data, green points represent SPICAM data, red points represent periapsis temperatures calculated from inbound legs of MRO/ACCEL data, and magenta represent those calculated from outbound legs. The cyan curves are the result of averaging the available MCS data over ½ °-Latitude bins. The sol-

id blue line tracks the migration of $T_{hemispheric\ max}$. In this representation, the increase in ΔT magnitude and the

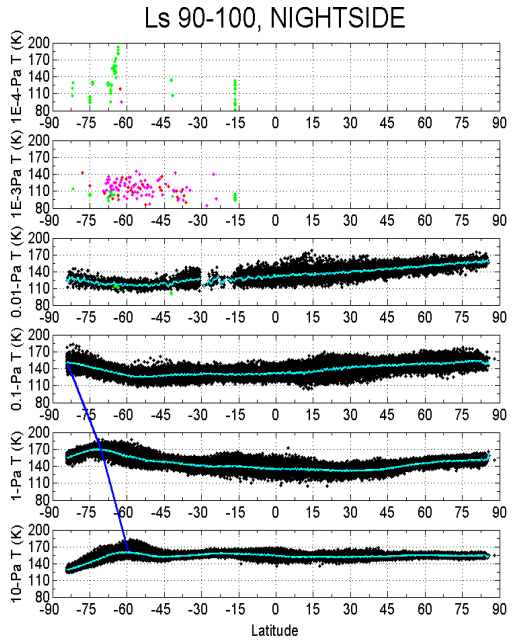

Figure 2. Nightside (LST = 1900 – 0500) observations on constant pressure-surfaces. See text for discussion.

pole-ward migration of $T_{hemispheric\ max}$ with decreasing pressure (from p = 10 Pa to $1x10^{-1}$ Pa) is clear. Also apparent from the cyan curves is the steepness of the reversed latitudinal temperature gradient, ∇T, from the equator to $T_{hemispheric\ max}$, on each constant-pressure surface. The SPICAM data shows signs of strong PW on the p = $1x10^{-4}$ Pa surface; however the data is sparse. There is no indication of PW in the MRO/ACCEL data.

Future Work: With nearly two full Martian years of MCS data available we are now able to characterize variations of PW with pressure, season, and MY. Future work includes validating the newly extended Mars-WRF GCM with the constraints presented in this study and implementing a gravity wave drag scheme to address some of the questions about PW formation posed above. Preliminary results from the Mars-WRF study are presented in a separate poster at this conference [15].

References: [1] Deming D. et al. (1986), *Icarus*, *66*, doi: 10.1016/0019-1035(86)90165-X. [2] Théodore B. et al. (1993), *Icarus, 105*, doi:10.1006/icar.1993.1145. [3] Santee M. and Crisp D. (1993), *J. Geophys. Res., 98,* doi: 10.1029/92JE01896. [4] Bougher S. W. et al. (2006), *Geophys. Res. Let., 33,* doi: 10.1029/2005GL024059. [5] Hartogh P. et al. (2007), *Planet. and Space Sci., 55,* doi: 10.1016/j.pss.2006.11.018. [6] McCleese D. et al. (2008), *Nature,* doi: 10.1038/ngeo332. [7] Kleinböhl A. et al. (2009), *J. Geophys. Res., 114,* doi: 10.1029/2009JE003358. [8] Forget F. et al. (2009), *J. Geophys. Res., 114,* doi: 10.1029/2008JE003086. [9] McCleese D. et al. (2010 submitted), *J. Geophys. Res.* [10] Wilson R. J. (1997), *Geophys. Res. Let., 24*, doi: 10.1029/96GL03814. [11] Forget F. et al. (1999), *J. Geophys. Res., 104,* doi: 10.1029/1999JE001025. [12] Bell J. et al. (2007), *J. Geophys. Res., 112, doi*: 10.1029/2006JE002856. [13] González□Galindo F. et al. (2009a), *J. Geophys. Res., 114*, doi: 10.1029/2008JE003277. [14] González□Galindo F. et al. (2009b), *J. Geophys. Res., 114*, doi: 10.1029/2008JE003246. [15] McDunn T. et al. (2010), *4th International Workshop on the Mars Atmosphere: modeling and observations. Paris, France.* Poster Presentation, "Modeling Polar Warming at Mars: Preliminary Results of the Newly Vertically Extended Mars-WRF GCM and Comparisons with Constraints from Data."